Published in final edited form as:
Mol Cancer Ther. 2013 August ; 12(8): 1471–1480. doi:10.1158/1535-7163.MCT-12-1227.

Novel Curcumin Loaded Magnetic Nanoparticles for Pancreatic Cancer Treatment

Murali M. Yallapu[1], **Mara C. Ebeling**[1], **Sheema Khan**[1], **Vasudha Sundram**[1], **Neeraj Chauhan**[1], **Brij K. Gupta**[1], **Susan E. Puumala**[2], **Meena Jaggi**[1,3], and **Subhash C. Chauhan**[1,3]

[1]Cancer Biology Research Center, Sanford Research/University of South Dakota

[2]Methodology and Data Analysis Center, Sanford Research/University of South Dakota

[3]OB/GYN, Basic Biomedical Science Division, Sanford School of Medicine, University of South Dakota, Sioux Falls, South Dakota

Abstract

Curcumin (CUR), a naturally occurring polyphenol derived from the root of *Curcuma longa*, has demonstrated potent anti-cancer and cancer prevention activity in a variety of cancers. However, the clinical translation of curcumin has been significantly hampered due to its extensive degradation, suboptimal pharmacokinetics and poor bioavailability. To address these clinically relevant issues, we have developed a novel curcumin loaded magnetic nanoparticle (MNP-CUR) formulation. Herein, we have evaluated the *in vitro* and *in vivo* therapeutic efficacy of this novel MNP-CUR formulation in pancreatic cancer. Human pancreatic cancer cells (HPAF-II and Panc-1) exhibited efficient internalization of the MNP-CUR formulation in a dose dependent manner. As a result, the MNP-CUR formulation effectively inhibited growth of HPAF-II and Panc-1 cells in cell proliferation and colony formation assays. The MNP-CUR formulation suppressed pancreatic tumor growth in an HPAF-II xenograft mice model and improved mice survival by delaying tumor growth. The growth inhibitory effect of MNP-CUR formulation was correlated with the suppression of PCNA, Bcl-xL, Mcl-1, MUC1, Collagen I and enhanced membrane β-catenin expression. MNP-CUR formulation did not show any sign of hemotoxicity and was stable after incubation with human serum proteins. Additionally, the MNP-CUR formulation improved serum bioavailability of curcumin in mice up to 2.5 fold as compared to free curcumin. Biodistribution studies demonstrate that a significant amount of MNP-CUR formulation was able to reach the pancreatic xenograft tumor(s) which suggests its clinical translational potential. In conclusion, this study suggests that our novel MNP-CUR formulation can be valuable for the treatment of pancreatic cancer.

Keywords

magnetic nanoparticles; curcumin; chemoprevention; pancreatic cancer; nanomedicine

Corresponding author: Subhash C. Chauhan, PhD Cancer Biology Research Center Sanford Research/University of South Dakota 2301 E. 60th Street North Sioux Falls, SD 57104-0589 Phone: 605-312-6106; Fax: 605-312-6071 Subhash.Chauhan@sanfordhealth.org.

Disclosure of Potential Conflicts of Interest: The authors report no conflicts of interest in this work

Authors' Contributions Conception and design: M.M. Yallapu, S.C. Chauhan, M. Jaggi; Development of methodology: M.M. Yallapu, S.C. Chauhan, M. Jaggi; Acquisition of data: M.M. Yallapu, M.C. Ebeling. S. Khan, V. Sundram, B.K. Gupta, N. Chauhan; Analysis and interpretation of data: M.M. Yallapu, S.C. Chauhan, S. Khan, V. Sundram, S.E. Puumala; Writing, review, and/or revision of the manuscript: M.M. Yallapu, S.C. Chauhan, S. Khan, V. Sundram, S.E. Puumala, M. Jaggi; Study supervision: S.C. Chauhan, M. Jaggi.

Introduction

Pancreatic cancer ranks fourth in causing cancer related deaths in the United States (1). Recent statistics estimated that 44,030 individuals were diagnosed with pancreatic cancer and 37,660 patients died in 2011 from this highly devastating disease (1). In spite of significant progress in the area of cancer therapeutics, pancreatic cancer still remains by and large untreatable with an extremely poor 5-year survival rate (1). Poor vasculature and the hyperfibrotic and desmoplastic tumor microenvironment of pancreatic cancer are primarily responsible for reduced uptake of chemotherapeutic drugs and low therapeutic outcome (2, 3). Gemcitabine is a standard chemotherapeutic drug used for the treatment of pancreatic cancer; however, survival is increased by only 5-12 months (4, 5). In addition, this therapeutic approach may lead to severe toxicity and may also result in chemo-resistance. Therefore, developing a safer and more efficient therapeutic modality to improve management of pancreatic cancer is highly desirable. Due to their potent anti-cancer activity, a few natural dietary ingredients are considered as complementary and alternative medicine by the National Cancer Institute for cancer prevention/treatment options. Treatment that can modulate tumor microenvironment using a natural dietary agent would be considered a novel therapeutic strategy.

Curcumin (chemical structure, Fig. 1A) is a widely known natural bioactive polyphenolic component of turmeric. Curcumin is also a “Generally Recognized As Safe” (GRAS) compound by the Food and Drug Administration (FDA) (6). Curcumin exhibits both anti-cancer and cancer prevention activities by suppressing key elements of initiation, promotion, and metastasis of a wide range of cancer(s) (7). The multi-targeting role of curcumin enables it to perform a wide spectrum of actions against cancer(s) (8). Epidemiological studies revealed that populations with curcumin consumption have lower incidence and risk of various types of cancers including pancreatic cancer (9-11). Because curcumin possesses exceptional therapeutic properties, more than 20 clinical trials are underway to assess curcumin’s efficacy in cancer treatment(s) (as of Jan. 2013). *In vitro* studies have concluded that curcumin exhibits anti-cancer effects at micromolar concentrations. However, achieving these concentrations at the tumor site in humans is highly challenging and has not yet been accomplished due to its higher metabolic activity and low bioavailability (10, 12). Curcumin nanoformulations can be a useful delivery module (12). Curcumin nanoformulations have demonstrated an enhanced delivery of curcumin in biologically active form to various cancer cells (13). While many nanotechnology investigations have primarily focused on either improving stability or bioavailability of curcumin, limited studies have been pursued related to therapeutic effects on pancreatic cancer (14-18). To date, no study has reported on magnetic nanoparticle mediated curcumin delivery for treatment of pancreatic cancer. Herein we report, for the first time, the effects of a novel curcumin loaded magnetic nanoparticle (MNP-CUR) formulation (Patent# PCTUS2011/063723) on human pancreatic cancer cells *in vitro* and *in vivo* and elucidate its potential translational capabilities. Additionally, we have used advanced and appropriate quantitative methods to study the efficacy of this novel formulation in both *in vitro* and xenograft mouse models.

Materials and methods

Chemicals, reagents, and antibodies

All chemicals and reagents were acquired from Sigma Aldrich Corporation and cell culture plastic ware and consumables were purchased from BD Biosciences, unless otherwise mentioned. The preparation and characterization of the MNP-CUR formulation was conducted following our optimized/patented composition protocol (19). Monoclonal antibodies against B-cell lymphoma-extra large (Bcl-xL) (Abcam), induced myeloid leukemia cell differentiation protein (Mcl-1) (Abcam), proliferating cell nuclear antigen

(PCNA) (Cell Signaling Technology), collagen I (Abcam), β-actin (Sigma), cell surface associated Mucin 1 (MUC1) (Cell Signaling Technology), and β-catenin (gift of Dr. Keith Johnson, University of Nebraska Medical Center, Omaha, Nebraska) were used for immunohistochemistry and Western blot analyses.

Cancer cell lines and animals

HPAF-II and Panc-1 human pancreatic cancer cell lines were purchased from American Type Cell Culture (ATTC), cultured as monolayer in 75 cm^2 culture flasks in DMEM-F12/DMEM medium (HyClone Laboratories, Inc.) and supplemented with 10% heat-inactivated fetal bovine serum (Atlanta Biologicals),1% penicillin and 1% streptomycin (Gibco BRL) at 37°C in a humidified atmosphere (5% CO2 and 95% air atmosphere). In order to maintain authenticity of the cell lines, frozen stocks were prepared from a parent stock and every six months a new frozen stock cell line was used for the experiments. All animal experiments were carried out using 6-8 week old male athymic nude/nude mice (Harlan Laboratories) and all procedures were approved by the Sanford Research/University of South Dakota Institutional Animal Care and Use Committee.

Cellular uptake

Cellular uptake of MNP-CUR formulation in HPAF-II and Panc-1 cancer cells was evaluated by Prussian blue stain and 1,10-phenanthroline photometric method. For the Prussian blue staining experiment, 2×10^5 cells were seeded in 6-well plates in 2 mL medium and cells were allowed to attach to the plates overnight. These cells were treated with 25-200 μg MNP-CUR formulation for 6 hours. After treatment, cells were washed (with PBS), fixed (with methanol), and incubated subsequently with a mixture of 2% potassium ferrocyanide, 2% hydrochloric acid for 30 minutes, and nuclear fast red-aluminum sulfate solution (0.1%) for 5-10 minutes at 25°C. The representative images of internalized MNP-CUR in cancer cells were captured at 20X magnification using an Olympus BX 41 Microscope (Olympus Corporation). For iron content estimation, pancreatic cancer cells (2×10^5) were treated with 100 μg MNP-CUR formulation, washed and trypsinized using 0.25% Trypsin-EDTA, and cell pellets were washed twice with 1X PBS, collected and dissolved in hydrochloric acid to determine iron content using 1,10-phenanthroline photometric method as described in our recent publications (19, 20).

Cell proliferation

Cells (5×10^4) were seeded in 6-well plates in 2 mL media and allowed to adhere overnight. Cells were then incubated with 5, 10 and 20 μM of free CUR or CUR equivalent MNP-CUR formulation for 2 days at 37°C. In this experiment, equivalent amounts of DMSO or MNPs (no curcumin) in PBS served as controls for CUR and MNP-CUR, respectively. The media was removed after 2 days, cells were washed with PBS, trypsinized and collected in culture medium and cell number was counted using a hemocytometer (21). Each concentration treatment was performed at least 6 times.

Clonogenic assay

Cells (500) were seeded in 6-well plates in 2 mL growth media and incubated for 2-3 days to allow grow into colonies. Cells were treated with 2, 4 and 8 μM free CUR or MNP-CUR for 7 days and then media without drugs for 7 days at 37°C. Subsequently, cells in all plates were gently rinsed with PBS, fixed with methanol and stained with hematoxylin. A population of at least 50 cells was considered a colony and the number of colonies was counted and quantified according to our standard previously reported protocol (22).

In vivo anti-tumor activity and survival study

Approximately 6-8 week old male athymic nude (nu/nu) mice were inoculated subcutaneously (s.c.) at their left flank with 5×10^6 HPAF-II human pancreatic cancer cells dispersed in a 200 μL solution of PBS and Matrigel (1:1 ratio; BD Biosciences) (21). These mice were used to evaluate both anti-tumor activity and survival analysis. On day 13 (post injection with cancer cells) the animals were randomly distributed into four groups (8 mice per group). Two treatment groups were administered intratumoral injections of 20 μg curcumin dissolved in 100 μL of 0.1% Tween 20 or 20 μg equivalent curcumin containing MNP-CUR dispersed in 100 μL PBS. Similarly, control groups were treated with either Tween 20 or empty MNPs (no curcumin). The tumor size was measured on day 7, 13, 20, 24, 28, 32, 35, and 40 using a digital Vernier caliper. The tumor size data was presented up to day 28 because of statistical analysis consideration. The tumor volume was calculated using the ellipsoid volume equation: tumor volume (mm^3) = $\pi/6 \times L \times W \times H$, wherein L is length, W is width, and H is height (21). The animals were sacrificed at the end of the treatment or when tumor volume reached 1000 mm^3. Survival of mice was followed until day 40 and a plot was generated using Origin 6.1 software. Tumor tissues were collected for immunohistochemical and immunofluorescence analyses as well as the analysis of MNP-CUR accumulation.

Immunohistochemical and immunofluorescence analyses

Immunohistochemical and immunofluorescence analyses were performed to investigate pathways that are involved in MNP-CUR mediated suppression of pancreatic tumor growth. For immunohistochemistry analysis, 10% formalin fixed tumor tissues were processed as described earlier (21, 23) and tissue slides were incubated with primary antibodies against Bcl-xL (1:400), Mcl-1 (1:300), PCNA (1:2000), β-catenin (1:200), and MUC1 (1:250). Protein expression was detected using MACH 4 Universal HRP Polymer detection kit (Biocare Medical) and 3,3′-diaminobenzidine (DAB substrate kit, Biocare Medical) as described earlier (21). Finally, slides were washed with water, counterstained with hematoxylin, dehydrated and mounted with Ecomount (Biocare Medical), immunostaining was assessed using an Olympus BX 41 Microscope (Olympus Corporation). Similarly for immunofluorescence analysis, rehydrated tissue slides were blocked using 4% normal donkey serum (Jackson ImmunoResearch Laboratories) followed by incubation with primary rat anti-mouse Collagen I (1:200; Chondrex, Inc) and mouse anti-human Collagen I (1:200; Abcam). After washing with PBS, tissue slides were incubated with secondary antibodies Alexa-Fluor 488 and Alexa-Fluor 568 (1:200) (Life Technologies). DAPI was used to visualize nuclei. A laser scanning confocal microscope (Nikon TIRF) was used with a 20X Apochromat objective and optical Z sections were taken at ~0.8 microns. Magnification, pinhole settings, laser and detector gains, which were set below saturation were identical across samples (21). Western blot experiments and analyses were followed as described earlier (19).

Accumulation of MNP-CUR in pancreatic tumors

Paraffin embedded tumor tissues were processed according to our protocol (21) and tissue sections were subsequently immersed in 10% potassium ferrocyanide and 10% hydrochloric acid solution for 20 minutes at 25°C and in 0.1% nuclear fast red-aluminum sulfate solution for 5 minutes at 25°C. Following dehydration, tissues were viewed and representative images captured at 40X magnification using an Olympus BX 41 Microscope.

Bioavailability studies of MNP-CUR formulation

To determine bioavailability of curcumin in blood serum in nu/nu mouse, 50 μg curcumin in Tween 20 or curcumin equivalent MNP-CUR formulation in PBS solution was administered

intraperitoneally (i.p.) using a 30G needle. At predetermined time intervals (5, 10, 15, 30, 60, 120, 360, 720 and 1440 min), blood was drawn from tails and serum was immediately collected by centrifugation at 2000 rpm for 5 minutes (Centrifuge 5415D, Eppendorf AG, Hamburg, Germany). Serum samples were stored at −80°C until further use. Serum samples (3-5 μL) were lyophilized using a Labconco Freeze Dry System (−48°C, 133 × 10^{-3} m Bar; Labconco) and curcumin was extracted from serum by incubating 2 days in acetonitrile. Curcumin concentrations were determined using an UltiMate high-performance liquid chromatography (Dionex Corporation) equipped with UltiMate 3000 injector, RS variable wavelength detector, and an Acclaim® polar advantage column of 3 μm 120 Å (4.6 × 150 mm). The mobile phase consisted of 1% citric acid:acetonitrile (50:50, v/v). Chromatograms were collected at 430 nm. Linear calibration curve for curcumin under similar conditions was obtained in the range of 1–10 ng/mL.

Biodistribution studies

To examine MNP-CUR biodistribution in different organs in mice, tumor bearing mice were injected intratumorally or intraperitoneally with 20 μg curcumin equivalent MNP-CUR formulations in 100 μL PBS solution using a 30G needle. After 24 hours, animals were euthanized and tumor, liver, spleen and brain tissues were collected and stored at −80°C. Tissue homogenates were prepared by grinding at 8000 rpm in PBS using a Power Gen 125 homogenizer (125 W, 115V, 50/60 Hz; Fisher Scientific) and lyophilized for quantitative analysis of iron of MNP-CUR. Known quantities of lyophilized tissue samples were dissolved in concentrated hydrochloric acid and iron content of MNPs was determined following 1,10-phenanthroline photometric method (24). The iron levels of control group mice (no MNP treatment) organs were subtracted to obtain absolute iron levels in tissues after treatment with MNP-CUR formulation. All organs were saved for Prussian blue staining analysis.

Protein adsorption

For this study, 1 mg of MNP-CUR formulation was incubated in 100 μg of fibrinogen, immunoglobulin G (IgG), transferrin or human serum albumin (HSA) solutions at 37°C. Within 2 hours of incubation, the plasma proteins formed a corona layer on each MNP-CUR nanoparticle. The adsorbed proteins on the MNP-CUR formulation were recovered by centrifugation at 12,000 rpm for 15 minutes, re-dispersed, and run for SDS-PAGE gel to quantify. Protocol for running gel, staining of protein with SimplyBlue™ SafeStain solution (Coomassie® G-250 stain; Life Technologies), and densitometry methods were followed as previously reported (25). The variation in nanoformulation structure was also examined using transmission electron microscope (TEM) before and after HSA incubation (25).

Hemocompatibility

To examine hemocompatibility of the MNP-CUR formulation, 12.25 μL human red blood cells (RBCs) in 100 μL RPMI-1640 (healthy male Donor # 53554, Registration # 2577632, Biological Specialty Corp, Colmar, PA) was incubated with 100 μg MNP-CUR at 37°C in Eppendorf tubes. After 2 hours of incubation, the RBCs were collected by centrifugation and observed for ultra structural morphologies using transmission electron microscopy (TEM). The no-treatment group and dendrimer formulations were used as negative and positive controls, respectively.

Statistical analyses

Descriptive data are presented as the mean ± standard error of the mean. ANOVA models and t-tests were used to evaluate differences in *in vitro* properties. Linear mixed regression analyses were performed to determine the tumor volumes as a function of time.

Transformations of continuous variables were performed to meet model assumptions. Time to death (or euthanization) was used for Kaplan–Meier analysis and equality of survival was determined using log-rank analysis. All analysis was performed using SAS 9.3 (SAS Institute, Inc). P values of < 0.05 were considered significant. All graphs were plotted using Origin 6.1 software.

Results

Optimal size of MNP-CUR formulation for cancer therapeutics

In this study we have investigated utilization of "triple crown magnetic nanoparticles" as a delivery vehicle for curcumin (MNP-CUR) (17). The optimized MNP-CUR was formulated with 810:300 mg Fe^{3+}:Fe^{2+} salts, 200 mg cyclodextrin (CD), 250 mg Pluronic F-127 (19) with 10 wt/wt.% CUR loading (Fig. 1A). An average individual MNP-CUR particle grain size of 10.5 ± 0.54 nm, observed under JEOL 1210 transmission electron microscopy (TEM; JEOL Ltd, Tokyo) (Fig. 1A), demonstrated the ultra small particle size nature of this formulation. However this formulation showed 109 nm particle size with - 0.99 mV zeta potential in dynamic light scattering (DLS) analysis (19). These nanoparticle characteristics are suitable for optimal cancer therapeutics purpose.

MNP-CUR effectively internalizes in pancreatic cancer cells

Qualitative analysis of Prussian blue staining in HPAF-II and Panc-1 cells showed a dose dependant uptake of MNP-CUR formulation (Fig. 1B). The uptake pattern was different in both cancer cells and this observation is consistent with uptake of other magnetic drug nanoformulations in cancer cells (26, 27). However, the amount of nanoparticle uptake in both cell lines was very close (i.e., 54.06% and 53.86%) when incubated with 100 μg of MNP-CUR formulation (Supplementary Fig. S1A).

MNP-CUR inhibits proliferation and clonogenic potential of pancreatic cancer cells

In cell proliferation experiments, curcumin and MNP-CUR exhibited a dose dependant inhibition of cell proliferation (Fig. 1C). At all three tested concentrations, MNP-CUR had a very similar cytotoxicity on cancer cells as compared to free curcumin treatment. This indicates the MNPCUR formulation preserved the inherent biological activity of curcumin. Additionally, the effect of MNP-CUR was tested in the colony formation assay using HPAF-II and Panc-1 pancreatic cancer cells. Curcumin and MNP-CUR formulation effectively inhibited the clonogenic potential of HPAF-II and Panc-1 cancer cells compared to control treated cells (Fig. 1D). In cell proliferation and colony formation assay, only ~53% internalized MNP-CUR and ~40% released curcumin from MNP-CUR (19) caused cytotoxicity equivalent to free curcumin.

MNP-CUR decreases tumor growth and improves survival of tumor bearing mice

In vivo therapeutic efficacy of free CUR and the MNP-CUR formulation was examined in the HPAF-II tumor xenograft model following intratumoral administration. After cancer cells post injection, on day 28, MNP-CUR treatment significantly inhibited tumor growth by 71.2**%** compared to empty MNP treated controls, whereas the treatment with curcumin inhibited tumor growth by 35.9**%** (Fig. 2A). Tumor size steadily increased in Tween 20 or MNP groups. A significant difference in tumor volume was observed for MNP vs. MNP-CUR ($p = 0.02$), but not for Tween 20 vs. curcumin (CUR) ($p = 0.30$). Higher tumor growth inhibition observed with MNP-CUR formulation may be attributed to long term sustained release of curcumin from MNPCUR formulation within tumors. It was evident from the uptake experiment using flow cytometer that the MNP-CUR formulation can provide higher concentrations of curcumin within cells compared to free curcumin (Supplementary Fig.

S1B). The flow cytometer measurements are based on the inherent fluorescence signals from the curcumin in solution or curcumin in nanoparticles. In order to prove that MNP-CUR remains in tumors after intratumoral injection and protects curcumin's biological activity, we examined the accumulation of MNP-CUR formulation on the histological sections of tumor tissues by Prussian blue staining. Distinct Prussian blue stains were found throughout the region of the tumor(s) (Fig. 2B a-e). Most of the tissues showed a similar pattern of Prussian blue staining but a few tumor slides revealed only peripheral stains (Fig. 2B f). The observed patterns of nanoparticle existence in tumors are in accordance with a previous study (25). The Kaplan-Meier curves of mice treated with Tween 20 or empty MNPs exhibited a lower survival rate, but this was not statistically significant (Fig. 2C). Median survival was 40 days for MNP and 24 days for Tween 20. Both the curcumin (CUR) and the MNP-CUR groups had survival rates above 0.5 by the end of the study period.

MNP-CUR formulation effectively modulates key oncogenic molecular targets

A markedly decreased (~70%) staining of Bcl-xL and Mcl-1 was observed in both curcumin and MNP-CUR treated animals compared to vehicle control groups (Fig. 3A). Interestingly, MNPCUR treated animals demonstrated relatively less PCNA staining (~75%) compared to free-curcumin (~55%). Additionally, we investigated the expression of a dual-function protein, β-catenin (a modulator of cell-cell adhesion and wnt signaling), in these tumor tissues. The deregulated expression or function of this protein results in decreased cell-cell adhesion due to loss of surface β-catenin and in enhanced cell proliferation due to the nuclear function of β-catenin as a co-transcription factor (16, 28). A distinct increase in membrane β-catenin was detected in MNP-CUR treated tumors (~80%) compared to free curcumin treated tumors (~60%) and control animals (Fig. 3A). MUC1 is a transmembrane O-glycosylated protein that is overexpressed in pancreatic cancer (29) and modulates various signaling pathways (including β-catenin), resulting in the overexpression of tumorigenic factors and formation of tumors. A striking downregulation (~75-80%) of MUC1 protein expression was observed upon curcumin or MNP-CUR treatment (Fig. 3A). These results were also observed *in vitro* in HPAF-II cancer cell line models (Fig. 3B). To elucidate the role of curcumin and MNP-CUR on tumor tissue fibrosis (desmoplasia), tumor tissues were double stained with anti-human collagen-1 (green) and anti-mouse collagen-1 (red). There was a marked reduction in both the human and mouse collagen levels in the tumors of mice treated with MNP-CUR (Fig. 4A) which implicated a decrease in host-tumor interactions. In vitro collagen production also significantly dropped to 24-25% upon treatment with MNP-CUR (Fig. 4B). Curcumin treatment did not efficiently regulate collagen production, i.e., collagen production was ~71-84%. All together, these data indicate an enhanced efficacy of MNP-CUR treatment at the molecular level compared to control and free curcumin.

MNP-CUR increases bioavailability and tumor targeting

Up to a 2.5-fold increase in bioavailability of CUR in blood plasma was observed with the MNPCUR formulation as compared to free curcumin (Fig. 5A). A considerable amount of CUR in MNP-CUR (1792.19 ± 644 ng) was observed in 1 mL serum at 6 hours while only 766.54 ± 256 ng of CUR in Tween 20 was present. This increased serum bioavailability implies greater stability and prolonged sustained blood circulation of MNP-CUR under physiological conditions (30, 31) demonstrating that magnetic nanoparticles possess strong properties as effective drug carriers.

To investigate key differences in biodistribution patterns of the MNP-CUR formulation injected intratumorally and intraperitoneally, the presence of MNPs was examined in tumor, liver, spleen and brain during the 24 hours after administration (Fig. 5B). Other organs, including pancreas, exhibited very minimal or undetectable levels of MNPs (data not

shown). Intratumoral administration obviously resulted in high concentrations of MNP-CUR in tumor (1.04 ±0.48 mg Fe/g tissue), followed by liver (0.39 ±0.17 mg Fe/g tissue), spleen (0.059 ±0.2 mg Fe/g tissue), and brain (0.14 ±0.02 mg Fe/g tissue). Interestingly, fairly high accumulation of MNP-CUR in tumor (0.48 ±0.29 mg Fe/g tissue) as well as in spleen (0.78 ±0.29 mg Fe/g tissue) was also achieved with i.p. administration. This observation was further confirmed by Prussian blue staining of tumor tissues. This data also indicate that MNP-CUR formulation is capable of targeting pancreatic tumors fairly well with the help of the "Enhanced Permeation and Retention" (EPR) effect even with systemic (i.p.) administration (Fig. 5C).

MNP-CUR interaction with plasma proteins and RBCs

SDS-PAGE revealed the following order of quantity of bound plasma proteins on MNP-CUR: Transferrin > HSA > fibrinogen > IgG (Supplementary Information 2). Relative protein binding quantification by densitometry showed the protein affinity towards nanoparticles (Fig. 6A). This order variation occurred due to differences in the formation of protein corona on nanoparticles that resulted from nanoparticle-protein complex interplay factors (32). A similar protein binding order had been noticed in curcumin assemblies (33). Human serum proteins have prevalent interactions with nanoparticles but higher aggregation of those complexes lead to opsonization; however, this was not observed with the MNP-CUR formulation.

Further, we compared the hemocompatibility of MNP-CUR formulation with human RBCs (100 μM curcumin equivalent MNP-CUR formulation) to negative control (no treatment) and positive control (dendrimer formulation) groups. RBCs treated with MNP-CUR retained their morphology similar to negative control RBCs (Fig. 6B). This behavior is achieved due to the pluronic layers (bound polyethylene glycol chains) in the formulation. However, some nonspecific binding of MNP-CUR with RBCs was also observed (Fig. 6B, black circle) which is due to entrapment of nanoparticles in the cell pellet. In contrast, the dendrimer formulation caused secretion of hemoglobin and membrane proteins due to compromised RBC membranes and hemolytic activity (Fig. 6B, black arrows).

Discussion

Our systematic approach for curcumin encapsulation in magnetic nanoparticles (MNP-CUR formulation) demonstrated minimized uptake in RAW 247.1 cells (macrophages) which can prevent rapid clearance while enhancing synchronized internalization in cancer cells (19) including pancreatic cancer cells (Fig. 1B). The MNP formulation is also able to encapsulate other clinically relevant drugs such as doxorubicin and gemcitabine without significantly altering their structure. Effective internalization of magnetic nanoparticles in cancer cells is an important characteristic for drug delivery. A layer of bio-adhesive material, Pluronic F127, on the magnetic nanoparticles greatly improved their cellular uptake and reduced particle aggregation (34). Sustained release of curcumin from magnetic nanoparticles will not only improve anti-cancer efficacy but also help prevent relapse and drug resistance (35). Herein, we report for the first time, the anti-tumor efficacy of an MNP-CUR formulation in pancreatic cancer treatment using *in vitro* (Fig. 1C-D) and *in vivo* (Fig. 2A-C) models. Such equivalent biological activities against various cancer cells were observed for drugs in solution and magnetic nanoparticle drug formulations (26, 36). As a drug carrier, MNPs can effectively increase the stability of drugs, protect them from degradation, promote targeting efficacy and reduce side effects. In this study, tumor growth inhibition was observed with a single dose administration of MNP-CUR formulation. A more significant therapeutic effect can be expected from a multiple dose treatment schedule for a longer duration. MNP-CUR treatment not only suppressed tumor growth (Fig. 2A) but also increased the survival of

animals in a pancreatic cancer xenograft mouse model (Fig. 2C). No signs of behavioral abnormalities, undesirable side effects or genotoxicity were observed during the course of treatment because MNPs are made with iron salts (Fe^{2+} and $Fe3^{+}$). Human pancreatic cancer is known to be sensitive to multiple chemotherapeutic agents but often develops drug resistance. Previous studies have shown injectable drug-gel formulations maintained high tumoral drug load concentrations compared to free drug solutions (37). Our study demonstrates that in a pancreatic cancer xenograft mouse model, human pancreatic tumors can retain the MNP-CUR formulation even after 2-3 weeks (Fig. 2B). Similar sustained release of curcumin was found at the site of injection of curcumin microparticles in mice (38). This data suggests the utility of our unique delivery vehicle to effectively deliver anti-cancer drugs to pancreatic tumors. These formulations can be used for intratumoral therapy through endoscopic ultrasound (EUS) procedures or percutaneously guided intratumoral injections to shrink the tumors and prevent tumor recurrence (39).

This study also suggests that the MNP-CUR formulation efficaciously decreased pancreatic tumor growth *via* alterations in the expression profiles of cell survival associated proteins (Fig. 3A). Interestingly, the MNP-CUR treated tumors exhibited higher levels of membrane β-catenin compared to control and free curcumin treatments (Fig. 3A). β-catenin is a well-known modulator of tumorigenesis (40). The deregulated expression or function of this protein results in decreased cell-cell adhesion due to loss of surface β-catenin and enhanced cell proliferation due to its increased nuclear transcriptional activity (22, 40). In fact, aberrant nuclear localization and expression of β-catenin has been considered to be one of the primary factors in pancreatic tumorigenesis (41). Additionally, researchers have confirmed that MUC1 overexpression, aberrant localization and abnormal post-translational modification (phosphorylation, hypo-glycosylation and sulphation) are highly associated with pancreatic cancer progression (29, 42). The intracellular, c-terminal portion of MUC1 plays a critical role in signal transduction by regulating various signaling pathways, including the β-catenin signal pathway. This in turn results in the transcription/ overexpression of pro-growth factors. In addition, MUC1 contains a large extracellular ectodomain that protrudes above the cell surface (200-2000 nm); hence overexpression or aberrant baso-lateral localization of MUC1 may also reduce cell-cell adhesion, thereby enhancing the tumorigenesis of pancreatic cancer (29, 43). CUR and MNP-CUR treatments decrease the levels of MUC1 in the tumor tissues and, therefore, possess a tumor-suppressing function by downregulating pro-survival proteins (Bcl-xL, Mcl-1 and PCNA) (Fig. 3A-B). Moreover, upon MNP-CUR treatment, the enhanced membranous β-catenin might enhance cell-cell adhesion within the tumor and prevent tumor metastasis. Therefore, a significant long term implication of decreased MUC1 expression and increased membranous β-catenin of the cells in the tumor may lower the risk of metastasis (a phenomenon that is primarily responsible for cancer related deaths).

The major extracellular matrix component produced by myofibroblasts, collagen I, not only functions as a scaffold for the tissue but also regulates the expression of genes associated with cellular signaling, metabolism, gene transcription and translation. Thus, production of collagen I affects fundamental cellular processes that are essential for tumor progression, such as cell survival, apoptosis and cellular invasion (44, 45). This data indicates that MNP-CUR efficiently inhibited the collagen I levels of both human and mouse origins within tumors (Fig. 4). This supports the finding that MNP-CUR induced a decrease in host-tumor interactions, thus may be involve in preventing pancreatic fibrosis.

The prolonged circulation time and an enhanced permeation and retention (EPR) effect of nanoformulations are general strategies used to target tumor(s). The MNP-CUR formulation demonstrated a 2.5-fold increase in curcumin concentration in serum (Fig. 5A). The preferential tumor accumulation of MNP-CUR (Fig. 5B-C) is anticipated due to leaky

vasculature and lack of a lymphatic system in tumors. It is possible to further improve the accumulation of the MNPCUR formulation by application of an external magnetic field gradient (46). Additionally, in this study we observed an appropriate binding of transferrin and HSA proteins to the MNP-CUR nanoparticles to form a “hard corona” (Fig. 6A) which defines the long-lived equilibrium state of novel MNP-CUR nanoparticles (47). In general, enhanced adsorption of plasma proteins onto the surface of nanoparticles would lead to opsonization due to aggregation. However, we did not observe any aggregation property of MNP-CUR nanoparticles and hemotoxicity, indicating a long-term circulation of particles in the blood (Fig. 6A). Our particles gained this specific property due to the poly(propylene oxide) chain anchoring on the MNP-CUR formulation that minimizes the shear forces when nanoparticles are exposed to biological fluids. This observation was further confirmed by hemocompatibility of our formulation by evaluating RBC’s ultra-structural morphology which suggested no signs of interaction of MNP-CUR with blood components and hemolysis (Fig. 6B).

Active and specific targeting of drug delivery systems has now become an interesting concept in cancer therapeutic research. The advantage of this MNP formulation is that curcumin or other anti-cancer drug(s) can be loaded into the layers of cyclodextrin and F127 polymer. In addition, pancreatic cancer can be specifically targeted using a novel anti-MUC13 monoclonal antibody. Most other curcumin nanoformulations either inefficiently load higher amounts of curcumin or lack targeting chemistry. Our recent study has shown an overexpression of MUC13 in pancreatic cancer (21). A MUC13 targeted nanoformulation may lead to specific targeting of pancreatic cancer and possibly enhance further tumor uptake, thereby improving the efficacy of chemotherapeutic drugs while preserving imaging properties for simultaneous real-time monitoring of the disease condition.

Conclusions

Our data demonstrate that our MNP-CUR formulation can be efficiently internalized in human pancreatic cancer cells and induce potent anti-cancer effects. The *in vivo* tumor growth inhibition and improved survival rate demonstrate that the MNP-CUR formulation has superior anti-cancer activity compared to free curcumin. Additionally, the MNP-CUR formulation has exhibited an enhanced serum bioavailability of curcumin along with appreciable tumor uptake and hemocompatibility. In conclusion, results presented in this study suggest that MNP-CUR is an excellent prospect for effective pancreatic cancer treatment/management due to enhanced bioavailability of curcumin and its multifocal therapeutic effects.

Supplementary Material

Refer to Web version on PubMed Central for supplementary material.

Acknowledgments

We thank Cathy Christopherson (Center for Health Outcomes and Prevention, Sanford Research/USD) for critically reading the manuscript and for editorial assistance. We also thank Ashley Miller (Methodology Data Analyst, Sanford Research/USD) and Nichole Bauer (Cancer Biology Research Center, Sanford Research/USD) for statistical analysis and cell counting experiments, respectively. The authors also acknowledge the Imaging, Molecular Pathology, Flow Cytometry and Tumor Biology Cores of Sanford Research which are supported by P20 GM103548-02 grant awarded to Dr. Keith Miskimins.

Grant Support This study was supported by Governor’s Cancer 2010, Department of Defense (PC073887), and the National Institutes of Health (RO1 CA142736 and U01 CA162106) to S.C. Chauhan and a pilot grant through P20 GM103548-02 to M.M. Yallapu.

References

1. Siegel R, Ward E, Brawley O, Jemal A. Cancer statistics, 2011: the impact of eliminating socioeconomic and racial disparities on premature cancer deaths. CA Cancer J Clin. 2011; 61:212–36. [PubMed: 21685461]
2. Whatcott, CJ.; Posner, RG.; Von Hoff, DD.; Han, H. Desmoplasia and chemoresistance in pancreatic cancer. In: Grippo, PJ.; Munshi, HG., editors. Pancreatic Cancer and Tumor Microenvironment. Trivandrum (India): 2012.
3. Bartholin, L. Pancreatic cancer and the tumor microenvironment: Mesenchyme's role in pancreatic carcinogenesis. In: Grippo, PJ.; Munshi, HG., editors. Pancreatic Cancer and Tumor Microenvironment. Trivandrum (India): 2012.
4. Mancuso A, Calabro F, Sternberg CN. Current therapies and advances in the treatment of pancreatic cancer. Crit Rev Oncol Hematol. 2006; 58:231–41. [PubMed: 16725343]
5. Ng J, Zhang C, Gidea-Addeo D, Saif MW. Locally advanced pancreatic adenocarcinoma: update and progress. JOP. 2012; 13:155–8. [PubMed: 22406589]
6. U.S. Food and Drug Administration. Food Additive Status List. Revised as of April 1 AahwafgscccC
7. Joe B, Vijaykumar M, Lokesh BR. Biological properties of curcumin-cellular and molecular mechanisms of action. Crit Rev Food Sci Nutr. 2004; 44:97–111. [PubMed: 15116757]
8. Maheshwari RK, Singh AK, Gaddipati J, Srimal RC. Multiple biological activities of curcumin: a short review. Life Sci. 2006; 78:2081–7. [PubMed: 16413584]
9. Sinha R, Anderson DE, McDonald SS, Greenwald P. Cancer risk and diet in India. J Postgrad Med. 2003; 49:222–8. [PubMed: 14597785]
10. Goel A, Kunnumakkara AB, Aggarwal BB. Curcumin as "Curecumin": from kitchen to clinic. Biochem Pharmacol. 2008; 75:787–809. [PubMed: 17900536]
11. Stan SD, Singh SV, Brand RE. Chemoprevention strategies for pancreatic cancer. Nat Rev Gastroenterol Hepatol. 2010; 7:347–56. [PubMed: 20440279]
12. Yallapu MM, Jaggi M, Chauhan SC. Curcumin nanoformulations: a future nanomedicine for cancer. Drug Discov Today. 2012; 17:71–80. [PubMed: 21959306]
13. Bansal SS, Goel M, Aqil F, Vadhanam MV, Gupta RC. Advanced drug delivery systems of curcumin for cancer chemoprevention. Cancer Prev Res (Phila). 2011; 4:1158–71. [PubMed: 21546540]
14. Bisht S, Feldmann G, Soni S, Ravi R, Karikar C, Maitra A. Polymeric nanoparticle-encapsulated curcumin ("nanocurcumin"): a novel strategy for human cancer therapy. J Nanobiotechnology. 2007; 5:3. [PubMed: 17439648]
15. Bisht S, Mizuma M, Feldmann G, Ottenhof NA, Hong SM, Pramanik D, et al. Systemic administration of polymeric nanoparticle-encapsulated curcumin (NanoCurc) blocks tumor growth and metastases in preclinical models of pancreatic cancer. Mol Cancer Ther. 2010; 9:2255–64. [PubMed: 20647339]
16. Dandawate PR, Vyas A, Ahmad A, Banerjee S, Deshpande J, Swamy KV, et al. Inclusion Complex of Novel Curcumin Analogue CDF and beta-Cyclodextrin (1:2) and Its Enhanced In Vivo Anticancer Activity Against Pancreatic Cancer. Pharm Res. 2012; 29:1775–86. [PubMed: 22322899]
17. Li L, Braiteh FS, Kurzrock R. Liposome-encapsulated curcumin: in vitro and in vivo effects on proliferation, apoptosis, signaling, and angiogenesis. Cancer. 2005; 104:1322–31. [PubMed: 16092118]
18. Zhang F, Koh GY, Jeansonne DP, Hollingsworth J, Russo PS, Vicente G, et al. A novel solubility-enhanced curcumin formulation showing stability and maintenance of anticancer activity. J Pharm Sci. 2011; 100:2778–89. [PubMed: 21312196]
19. Yallapu MM, Othman SF, Curtis ET, Gupta BK, Jaggi M, Chauhan SC. Multi-functional magnetic nanoparticles for magnetic resonance imaging and cancer therapy. Biomaterials. 2011; 32:1890–905. [PubMed: 21167595]

20. Yallapu MM, Foy SP, Jain TK, Labhasetwar V. PEG-functionalized magnetic nanoparticles for drug delivery and magnetic resonance imaging applications. Pharm Res. 2010; 27:2283–95. [PubMed: 20845067]
21. Chauhan SC, Ebeling MC, Maher DM, Koch MD, Watanabe A, Aburatani H, et al. MUC13 mucin augments pancreatic tumorigenesis. Mol Cancer Ther. 2012; 11:24–33. [PubMed: 22027689]
22. Sundram V, Chauhan SC, Ebeling M, Jaggi M. Curcumin attenuates beta-catenin signaling in prostate cancer cells through activation of protein kinase D1. PLoS One. 2012; 7:e35368. [PubMed: 22523587]
23. Chauhan SC, Vannatta K, Ebeling MC, Vinayek N, Watanabe A, Pandey KK, et al. Expression and functions of transmembrane mucin MUC13 in ovarian cancer. Cancer Res. 2009; 69:765–74. [PubMed: 19176398]
24. Sandell, EB. Colorimetric Determination of Traces of Metals. 3rd Ed. Interscience Publishers Inc; New York: 1959.
25. Yallapu MM, Ebeling MC, Chauhan N, Jaggi M, Chauhan SC. Interaction of curcumin nanoformulations with human plasma proteins and erythrocytes. Int J Nanomedicine. 2011; 6:2779–90. [PubMed: 22128249]
26. Jain TK, Richey J, Strand M, Leslie-Pelecky DL, Flask CA, Labhasetwar V. Magnetic nanoparticles with dual functional properties: drug delivery and magnetic resonance imaging. Biomaterials. 2008; 29:4012–21. [PubMed: 18649936]
27. Cheng J, Cheng L, Chen B, Xia G, Gao C, Song H, et al. Effect of magnetic nanoparticles of Fe(3)O(4) and wogonin on the reversal of multidrug resistance in K562/A02 cell line. Int J Nanomedicine. 2012; 7:2843–52. [PubMed: 22745547]
28. Yamauchi J, Kanai M, Matsumoto S, Nishimura T, Yazumi S, Kami K, et al. Clinical outcome of gemcitabine/S-1 combination therapy for advanced pancreatic cancer. Pancreas. 2008; 36:327–8. [PubMed: 18362852]
29. Jonckheere N, Skrypek N, Seuningen IV. Mucins and Pancreatic Cancer. Cancers. 2010; 2:1794–812. [PubMed: 24281201]
30. Xie X, Tao Q, Zou Y, Zhang F, Guo M, Wang Y, et al. PLGA nanoparticles improve the oral bioavailability of curcumin in rats: characterizations and mechanisms. J Agric Food Chem. 2011; 59:9280–9. [PubMed: 21797282]
31. Kanai M, Imaizumi A, Otsuka Y, Sasaki H, Hashiguchi M, Tsujiko K, et al. Dose-escalation and pharmacokinetic study of nanoparticle curcumin, a potential anticancer agent with improved bioavailability, in healthy human volunteers. Cancer Chemother Pharmacol. 2012; 69:65–70. [PubMed: 21603867]
32. Cedervall T, Lynch I, Lindman S, Berggard T, Thulin E, Nilsson H, et al. Understanding the nanoparticle-protein corona using methods to quantify exchange rates and affinities of proteins for nanoparticles. Proc Natl Acad Sci U S A. 2007; 104:2050–5. [PubMed: 17267609]
33. Leung MH, Kee TW. Effective stabilization of curcumin by association to plasma proteins: human serum albumin and fibrinogen. Langmuir. 2009; 25:5773–7. [PubMed: 19320475]
34. Batrakova EV, Li S, Brynskikh AM, Sharma AK, Li Y, Boska M, et al. Effects of pluronic and doxorubicin on drug uptake, cellular metabolism, apoptosis and tumor inhibition in animal models of MDR cancers. J Control Release. 2010; 143:290–301. [PubMed: 20074598]
35. Das M, Sahoo SK. Folate decorated dual drug loaded nanoparticle: role of curcumin in enhancing therapeutic potential of nutlin-3a by reversing multidrug resistance. PLoS One. 2012; 7:e32920. [PubMed: 22470431]
36. Dilnawaz F, Singh A, Sahoo SK. Transferrin-conjugated curcumin-loaded superparamagnetic iron oxide nanoparticles induce augmented cellular uptake and apoptosis in K562 cells. Acta Biomater. 2012; 8:704–19. [PubMed: 22051236]
37. Smith JP, Kanekal S, Patawaran MB, Chen JY, Jones RE, Orenberg EK, et al. Drug retention and distribution after intratumoral chemotherapy with fluorouracil/epinephrine injectable gel in human pancreatic cancer xenografts. Cancer Chemother Pharmacol. 1999; 44:267–74. [PubMed: 10447573]

38. Shahani K, Swaminathan SK, Freeman D, Blum A, Ma L, Panyam J. Injectable sustained release microparticles of curcumin: a new concept for cancer chemoprevention. Cancer Res. 2010; 70:4443–52. [PubMed: 20460537]
39. Hecht JR, Farrell JJ, Senzer N, Nemunaitis J, Rosemurgy A, Chung T, et al. EUS or percutaneously guided intratumoral TNFerade biologic with 5-fluorouracil and radiotherapy for first-line treatment of locally advanced pancreatic cancer: a phase I/II study. Gastrointest Endosc. 2012; 75:332–8. [PubMed: 22248601]
40. Jaggi M, Chauhan SC, Du C, Balaji KC. Bryostatin 1 modulates beta-catenin subcellular localization and transcription activity through protein kinase D1 activation. Mol Cancer Ther. 2008; 7:2703–12. [PubMed: 18765827]
41. Morris, JPt; Wang, SC.; Hebrok, M. KRAS, Hedgehog, Wnt and the twisted developmental biology of pancreatic ductal adenocarcinoma. Nature reviews Cancer. 2010; 10:683–95.
42. Roy LD, Sahraei M, Subramani DB, Besmer D, Nath S, Tinder TL, et al. MUC1 enhances invasiveness of pancreatic cancer cells by inducing epithelial to mesenchymal transition. Oncogene. 2011; 30:1449–59. [PubMed: 21102519]
43. Kufe DW. Mucins in cancer: function, prognosis and therapy. Nature reviews Cancer. 2009; 9:874–85.
44. Zidar N, Gale N, Kambic V, Fischinger J. Proliferation of myofibroblasts in the stroma of epithelial hyperplastic lesions and squamous carcinoma of the larynx. Oncology. 2002; 62:381–5. [PubMed: 12138247]
45. Armstrong T, Packham G, Murphy LB, Bateman AC, Conti JA, Fine DR, et al. Type I collagen promotes the malignant phenotype of pancreatic ductal adenocarcinoma. Clin Cancer Res. 2004; 10:7427–37. [PubMed: 15534120]
46. Polyak B, Friedman G. Magnetic targeting for site-specific drug delivery: applications and clinical potential. Expert opinion on drug delivery. 2009; 6:53–70. [PubMed: 19236208]
47. Dell'Orco D, Lundqvist M, Oslakovic C, Cedervall T, Linse S. Modeling the time evolution of the nanoparticle-protein corona in a body fluid. PLoS One. 2010; 5:e10949. [PubMed: 20532175]

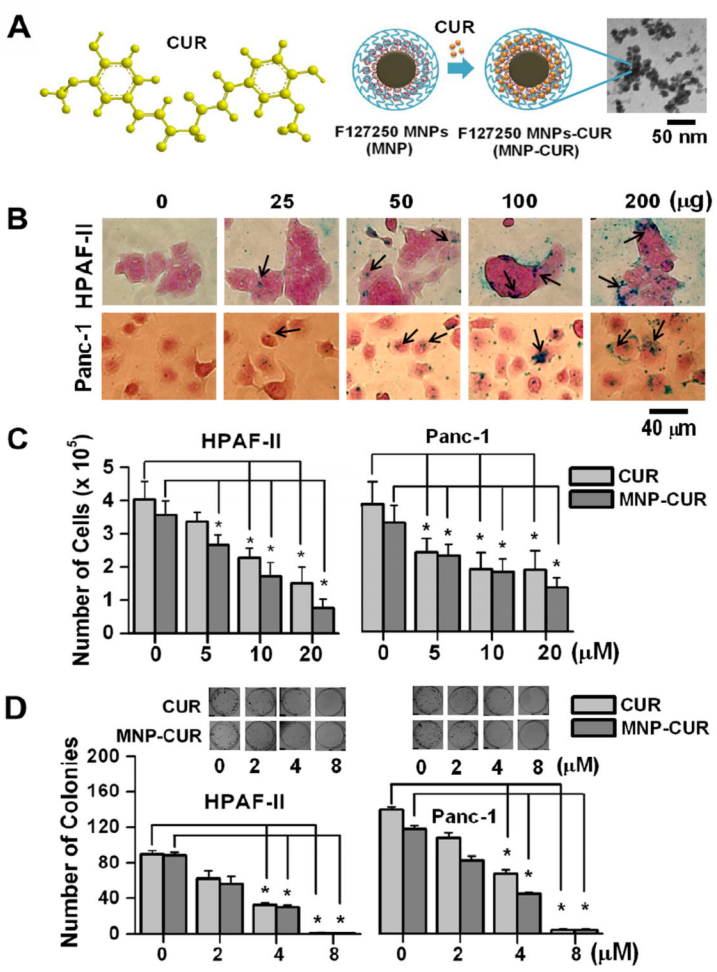

Figure 1.

MNP-CUR formulation efficiently internalizes and exhibits anti-cancer activity in pancreatic cancer cells. (A) Schematic representations of curcumin's chemical structure and MNP-CUR nanoformulation and a transmission electron microscope (TEM) image of MNP-CUR formulation (10.5 ± 0.54 nm, calculated from 20 randomly chosen nanoparticles using ImageJ Software). (B) MNP-CUR nanoformulation cellular internalization in pancreatic cancer cells. Cancer cells (2×10^5) were treated with a 25-200 μg MNP-CUR formulation for 6 hours and then processed for Prussian blue staining. Prussian blue stains in cancer cells are identified with black arrows. (C) The anti-cancer effects of curcumin (CUR) and MNP-CUR on HPAF-II and Panc-1 cancer in cell proliferation assays. Cancer cells were treated with 5-20 μM CUR/MNPCUR for 2 days, washed with PBS, trypsinized, and cell number was counted using a hemocytometer. Number of cells were counted in at least 6 treatments for each concentration and presented as mean ± SEM. (D) Effects of curcumin (CUR) and MNP-CUR on the growth of pancreatic cancer cells in colony formation assays. Cancer cells were treated with 2-8 μM CUR/MNP-CUR for 7 days, followed with a medium without CUR/MNP-CUR for 7 days. The colonies were rinsed with PBS, fixed with methanol, and stained with hematoxyline. Representative colony images are presented as inserts in graph. Note: Zero (0) on X-axis for cell proliferation and colony formation represents controls for CUR and MNP-CUR, respectively. The number of colonies was counted manually. Data represent mean ± SEM of triplicate procedures, $*P < 0.05$.

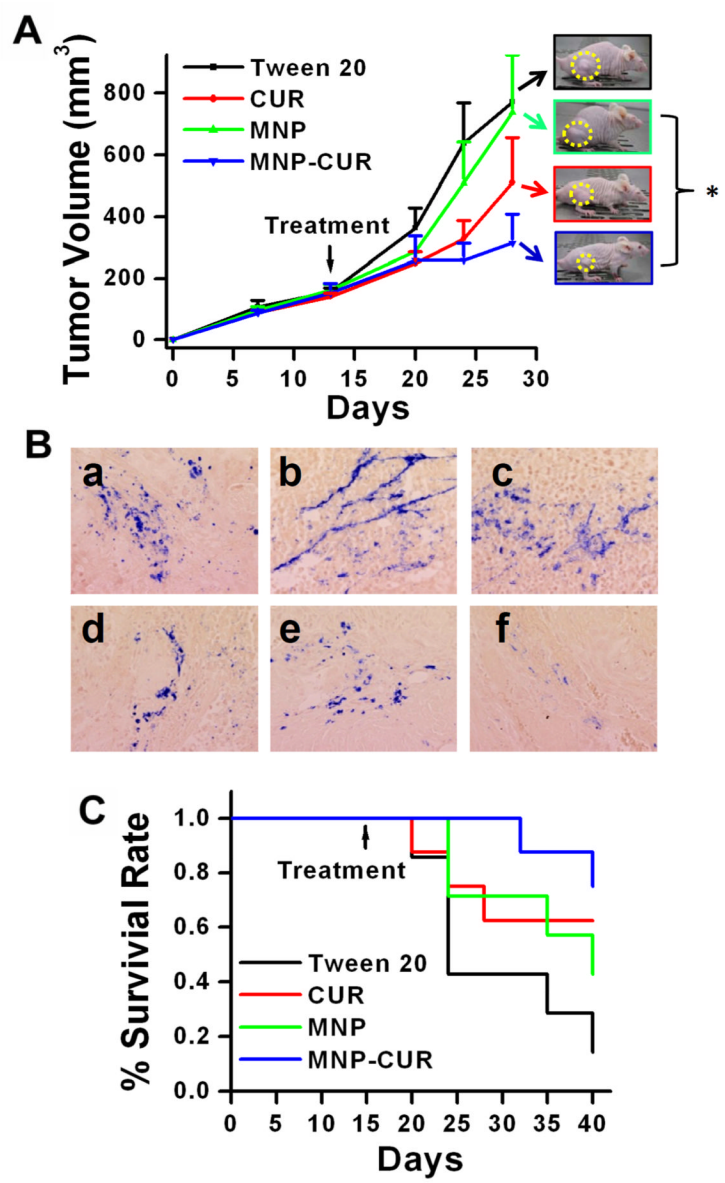

Figure 2.

MNP-CUR formulation efficiently inhibits tumor growth and increases survival of HPAF-II tumor xenograft bearing mice. (A) Single time intratumoral dose of MNP-CUR (20 μg in PBS) more efficiently inhibited growth of HPAF-II tumor xenografts as compared to free curcumin (20 μg in Tween 20) and controls (blank MNPs and Tween 20). Representative photographs of tumor bearing mice are shown as inset. (B) Photomicrographs of MNP-CUR treated tumors that were processed for Prussian blue staining. (C) Kaplan–Meier survival plot of mice treated with Tween 20, MNPs, curcumin (CUR) and MNP-CUR. Data represents at least 6 mice/group (Mean ± SEM), $*P < 0.05$.

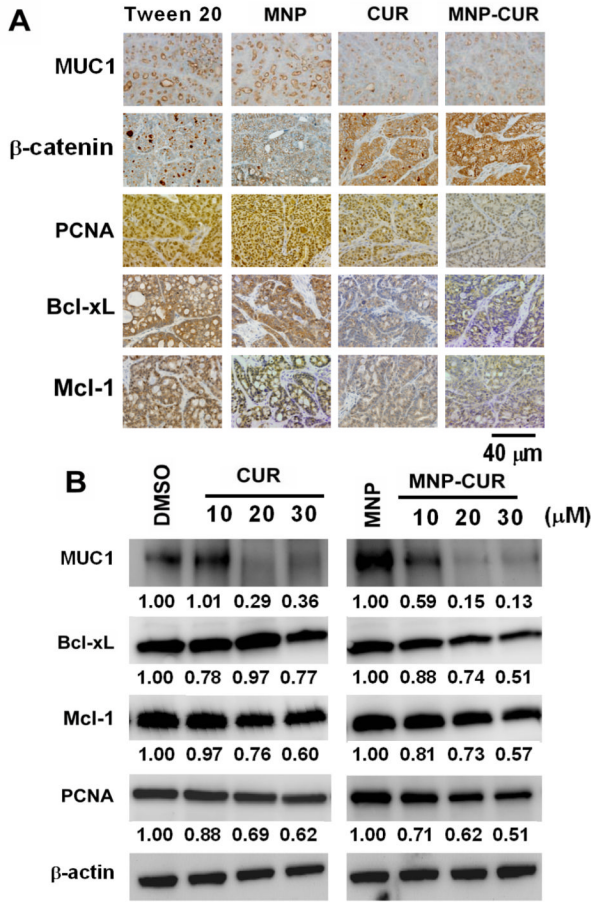

Figure 3.

Effects of curcumin (CUR) and MNP-CUR treatment on the expression of cell proliferation, cell survival and cell-cell adhesion molecules. (A) The expression of PCNA, Bcl-xL, Mcl-1, MUC1 and β-catenin in HPAF-II pancreatic tumor xenografts after treatment with an intratumoral injection of CUR/MNP-CUR (20 μg/mice). Representative images were obtained using an Olympus BX 41 Microscope. MNP-CUR treatment suppressed expression of pro-survival proteins (PCNA, Bcl-xL, Mcl-1 and MUC1) and enhanced membrane β-catenin localization compared to control treatment tumors. (Original Magnification 400X). (B) Cancer cells were treated with curcumin (CUR) or MNP-CUR (10-30 μM) for 36 hours and protein lysates were collected and the expression of PCNA, Bcl-xL, Mcl-1, and MUC1 proteins was analyzed by immunoblotting. β-actin was used as the loading control. DMSO and blank MNPs served as controls for curcumin (CUR) and MNP-CUR, respectively. The levels of each protein change are quantified using AlphaEase Fc software and relative data is normalized with respect to β-actin levels and included under each blot, considering control as 1.0.

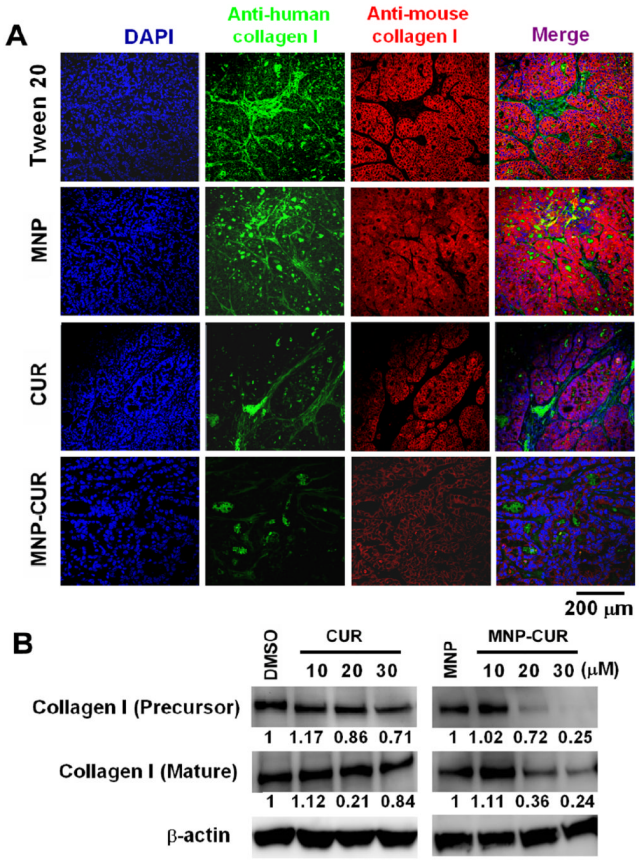

Figure 4.

Effect of curcumin (CUR) and MNP-CUR on Collagen I synthesis in pancreatic tumor xenografts. (A) HPAF-II tumor xenografts were double stained with anti-human collagen I (green) and anti-mouse collagen I (red). MNP-CUR treatment showed a marked decrease in both human and mouse collagen I levels in confocal microscopy analysis. (B) HPAF-II cancer cells were treated with curcumin (CUR) or MNP-CUR (10-30 μM) for 36 hours and protein lysates were collected and the expression of collagen I (mature and precursor) was analyzed by immunoblotting. β-actin was used as the loading control. DMSO and blank MNPs served as controls for curcumin (CUR) and MNP-CUR, respectively.

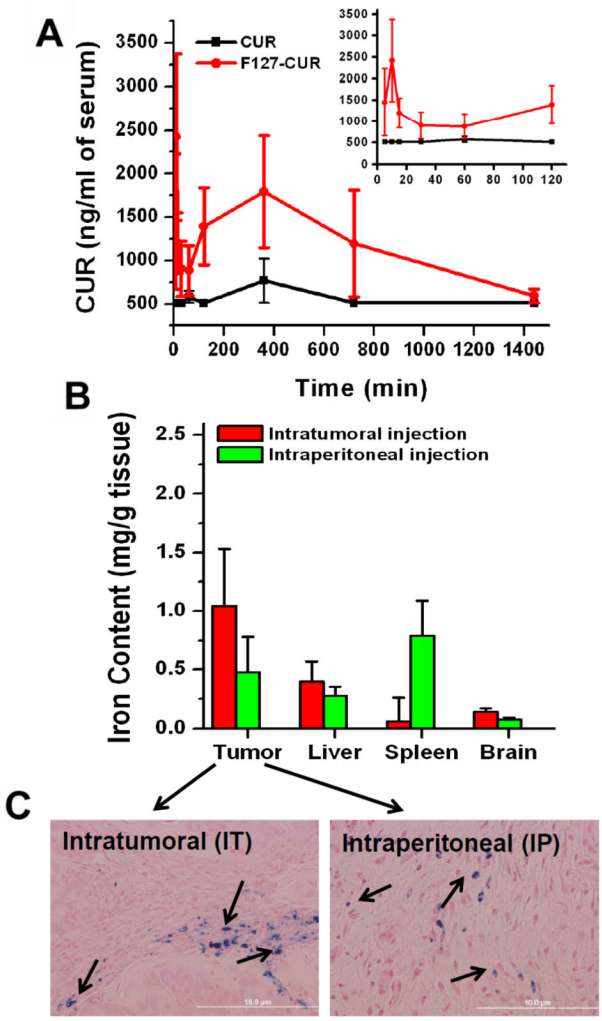

Figure 5.

Serum bioavailability and biodistribution of MNP-CUR formulation. (A) Comparative serum bioavailability of curcumin (CUR) and MNP-CUR formulations in a tumor bearing mice model. Enlarged 5, 10, 15, 30, 60 and 120 min bioavailability data is shown as inset. Curcumin (CUR) and MNP-CUR (50 μg per mice) were administered *via* intraperitoneal injection and blood samples from tail bleed were collected at different time points. CUR levels in serum was determined using a Dionex HPLC instrument equipped with an Acclaim Polar Advantage II C18 column (3 μm 120 Å 4.6 × 150 mm) with the RS variable wavelength detector at 420 nm. (B) Comparative biodistribution in tumor, liver, spleen and brain tissues after intratumoral and intraperitoneal administration of MNP-CUR formulation. Mice were treated with MNP-CUR particles (20 μg per mice) and iron content of particles in tissue was estimated using 1,10-phenanthroline colorimetric method. (C) Visual evidence of nanoparticles in tumor tissue was detected with Prussian blue staining method. Images were captured using an Olympus 1X71 microscope equipped with a DP71 camera (Olympus).

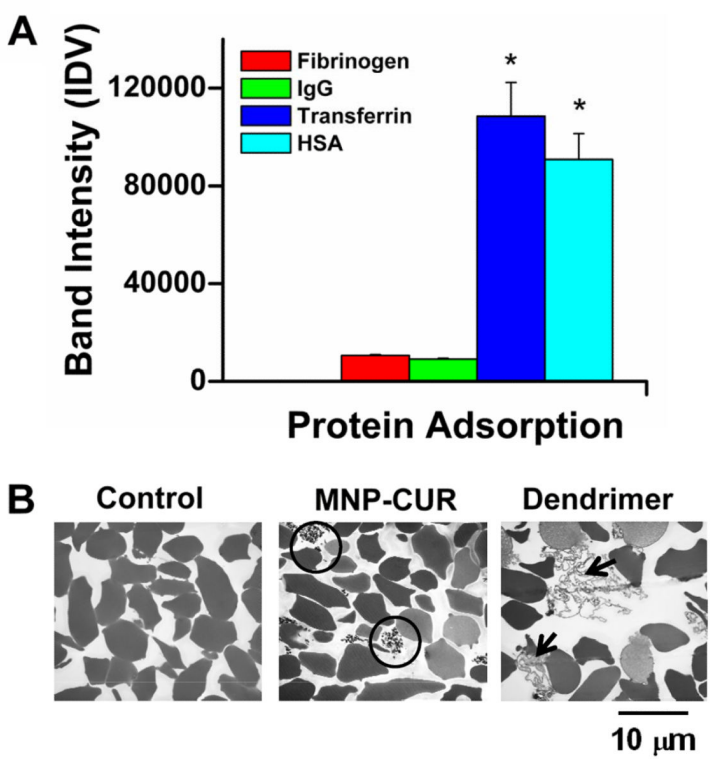

Figure 6.

Hemocompatibility of MNP-CUR formulation. (A) Serum proteins adsorption of MNP-CUR formulation. MNP-CUR formulation (1 mg) was incubated with 100 μg plasma proteins (fibrinogen, IgG, transferrin and HAS) for 2 hours, centrifuged, and bound proteins on NPs (palette) were estimated with the help of SDS-PAGE and Coomassie® G-250 staining (Supplementary Information Figure S2). Relative adsorbed protein density was quantified by densitometry using AlphaEase Fc software and data is presented as the mean of three repeats for each protein (Mean ± SEM). *$P < 0.05$ compared with Fibrinogen and IgG. (B) Morphological observation of red blood cells (RBCs) upon treatment with MNP-CUR formulation. Control RBCs and RBCs treated with dendrimer formulation were considered to be negative and positive controls for hemolysis, respectively. TEM images of RBCs reveal bound/entrapped MNP-CUR nanoparticles (black circle in MNP-CUR) and secreted proteins and membrane damage (black arrows in dendrimer treated group).